Computers and Concrete, Vol. 5, No. 6 (2008) 545-558
DOI: http://dx.doi.org/10.12989/cac.2008.5.6.545

Analysis on IBEM for consideration on reinforced concrete slab resistance

Je-Woon Kyung

Construction Division 1, Korea Institute of Construction & Transportation Technology Evaluation and Planning (KICTEP), 1600 Kwangyang-dong, Dongan-gu, Anayng-si, Gyeonggi-do, 431-060, Korea

Sung-Ho Tae* and Han-Seung Lee

School of Architecture & Architectural Engineering, Hanyang University 1271, Sa-1dong, SangNokgu, Ansan, Gyunggido, 425-791, Korea

Sung-Bok Lee

Housing and Urban Research Institute, Korea National Housing Corporation 175 Gumi-dong, Seongnam-si, Gyeonggi-do, 463-704 Korea

(Received November 5, 2007, Accepted October 14, 2008)

Abstract. The corrosion of RC structures demonstrates very complicated forms of deterioration intermingled together but all pointing to a decrease in the durability of RC structures due to the corrosion of reinforcing bars. Until now, nondestructive techniques, such as half-cell potential and polarization resistance, have been widely available in the world. The former provides information on the probability of corrosion while the latter is associated with information concerning corrosion rates. Inversion by the boundary element method (IBEM) was developed for considering concrete resistivity. The applicability of the procedure was examined through a numerical analysis and electrolytic tests for RC slabs. A distribution in such concrete resistivity is relatively inhomogeneous including cracks on the surface of slabs. Regarding cracks in concrete, the relative coefficient of concrete resistance was introduced to perform its analysis. Further, the procedure will be developed to identify the corroded region visually using 3-D VRML.

Keywords: half-cell potential; BEM; concrete resistivity; corrosion; corrosion area; VRML.

1. Introduction

The corrosion of RC structures demonstrates very complicated forms of deterioration intermingled together but all pointing to a decrease in the durability of RC structures due to the corrosion of reinforcing bars (Lee, *et al.* 2003, Okada, *et al.* 1998, Maruel, 2005, Tae, *et al.* 2007). There are major concerns in durability because carbon dioxide and chloride can penetrate concrete due to its porous nature (Andrade, *et al.* 2001). Furthermore, the economic impact has also become a major concern (Fontana, 1987). As a result, the passivity of steel is destroyed, and then rebars in concrete

* Corresponding Author, E-mail: jnb55@hanyang.ac.kr

are corroded. Until now, nondestructive techniques, such as half-cell potential and polarization resistance, have been widely available in the world. The former provides information on the probability of corrosion while the latter is associated with information concerning corrosion rates (Dubravka, *et al.* 2000).

An essential drawback of the half-cell potential measurement results from the fact that the potential is not measured at near rebars but on concrete surfaces. One way to compensate for this is to measure the potential at the most closed rebars in order to embed electrodes inside concrete or insert electrodes into the bottom of boreholes (Joggi, *et al.* 2001, Hiepas, *et al.* 2005). The other way to compensate for this is to determine the potential around rebars analytically. Potential distribution and current flow during a corrosion process can be formulated by numerical techniques, such as the finite element method (FEM), the finite difference method (FDM), and the boundary element method (BEM) (Jaggi, *et al.* 2001). The BEM analysis seems to be the most effective way for such corrosion problems because the quantity on the surface are only concerned.

In the present paper, a simplified inversion using the BEM analysis was applied to convert the potential on concrete surface to those on rebars taking into account cracks in concrete, the relative coefficient of concrete resistance was used in the analysis (Kyung, *et al.* 2005, Kyung, *et al*. 2007).

The applicability of the procedure was examined through accelerated corrosion tests for RC slabs. Further, the procedure was developed where results of IBEM were visualized by VRML (Virtual Reality Modeling Language) in 3-D space (Chris, *et al.* 1997. Hartman, 1996).

2. Analysis theory

2.1. Half-cell potential measurement

In the half-cell potential measurement, electric potential u in domain D (concrete) is measured at the surface. The potential in concrete satisfies the following Laplace equation,

$$\nabla^2(u/R) = 0 \quad \text{in} \quad D \tag{1}$$

where ∇ is a gradient (nabla) operator, and R is concrete resistivity. In a homogeneous body, R is a constant, and Eq. (1) becomes,

$$\nabla^2 u = 0 \quad \text{in} \quad D \tag{2}$$

As shown in Fig. 1, concrete is classified into four boundaries; Sp, So, Sc, and So. A specific

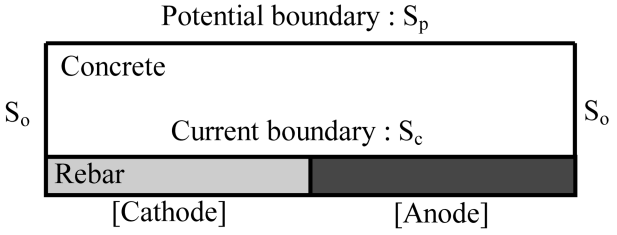

Fig. 1 Boundary conditions of concrete under corrosion

concrete surface in which potentials are measured corresponds to the potential boundary, Sp. Another boundary, So, is electrically free when the outward flow of currents is equal to zero.

The other is the current boundary, Sc, that represents the interface between concrete and rebars, consisted of anode and cathode regions. These boundary conditions are given as,

$$u = E(C.S.E) \text{ on Sp} \tag{3}$$

$$\partial(u/R)\partial n = 0 \quad \text{on} \quad \text{So} \tag{4}$$

$$\partial(u/R)\partial n = f \quad \text{on} \quad \text{Sc.} \tag{5}$$

Here, the potential, E, is measured using a copper-copper sulfate half-cell electrode, ($C.S.E$), and n is the outward normal vector to the surface. Also, f is the current flow at the interface boundary, Sc.

2.2. Inversion by BEM (IBEM)

As provided the concrete is referred as homogeneous, the solution $u(x)$ at point x can be solved by the boundary element method (BEM) (Brebbia 1978) :

$$\frac{1}{2}u(x) = \int_S \left[G(x,y)\frac{\partial u}{\partial n}(y) - \frac{\partial G}{\partial n}(x,y)u(y) \right] dS \tag{6}$$

where S is Sp + So +Sc, and y is located on the boundary, S, surrounding the domain concrete.

$G(x, y)$ is the fundamental solution:

$$G(x,y) = 1/4\pi r \text{ in the three-dimensional (3-D) body,} \tag{7}$$

where r is distance between x and y.

The boundary is discretized into boundary meshes, prescribing potential u_j and current $\partial u_j/\partial n$ at point x_j on a boundary mesh. Digitizing Eq. (6), a set of linear algebraic equations are obtained:

$$\sum_{j=1}^{N}\left[\frac{\delta_{ij}}{2} - \frac{\partial G_{ij}}{\partial n}\right]\{u_j\} = \sum_{j=1}^{N}[G_{ij}]\left\{\frac{\partial u_j}{\partial n}\right\} \qquad (i= 1,N) \tag{8}$$

where N is numbers of boundary meshes, δ_{ij} is Kronecker's delta symbol, and G_{ij} is Digitized fundamental solution between points x_i and x_j.

In the BEM, the internal potentials $u(x)$ are determined by,

$$u(x) = \int_{S_c} G(x,y)\left(\frac{\partial u}{\partial n}(y)\right) dS - \int_{S_p}\left(\frac{\partial G}{\partial n}(x,y)\right)u(y)dS \tag{9}$$

By applying Eq. (9) to an inverse solution at point x_i, which is located at the interface with rebars, the following equation is obtained as a digital form:

$$u_j = \sum_{j=1}^{M}\left[-\frac{\partial G_{ij}}{\partial n}\right]u_j \Delta S \tag{10}$$

Here, the current boundary, Sc, is neglected because $\partial u(y)/\partial n$ is always equal to zero, and the potential boundary, Sp, to be measured is divided into M rectangular elements in the area ΔS. As shown in Fig. 2, the measuring point of x_j at the center of the element is marked, and the potential u_j is measured at each location from No. 1 to No. 45. Potentials at the interface with the rebars, u_i,

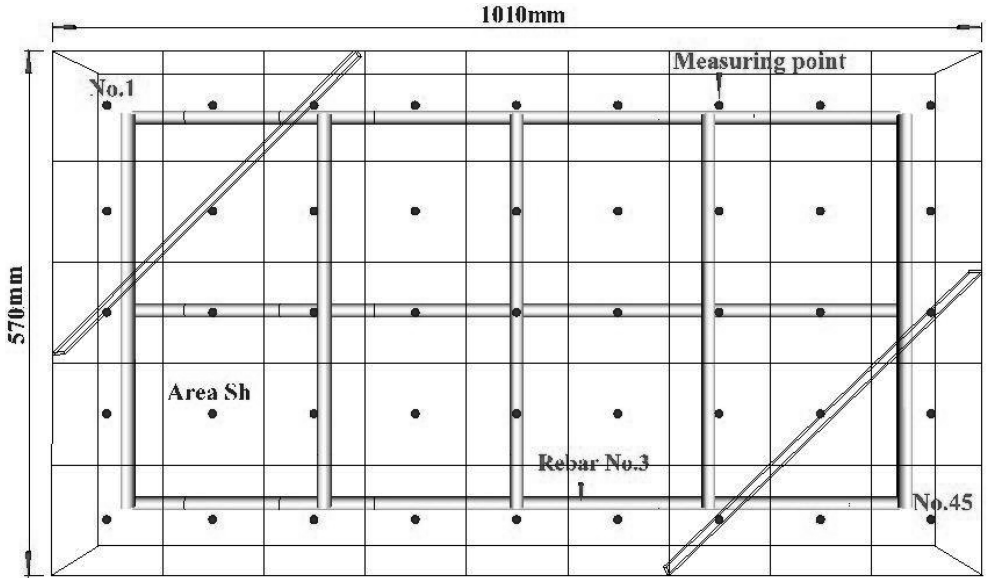

Fig. 2 Configuration of RC slab with surface cracks and measuring points

are computed as internal potentials, substituting potentials u_j, and area ΔS into Eq. (10).

The procedure is simple enough to implement readily in a microcomputer. Hereinafter, the potential at the interface with the rebars is referred to as those on the rebars. Furthermore, to take into account the concrete resistivity, Eq. (10) was modified:

$$u_i = \sum_{j=1}^{M} \left[-\frac{\partial G_{ij}}{\partial n} R \right] u_j \Delta S \tag{11}$$

where R is the relative coefficient of concrete resistivity.

Distribution of the resistivity is relatively inhomogeneous:

$$R = R_{ave} / R_p \tag{12}$$

where R_{ave} is the averaged concrete resistivity of the surface [kΩ]. R_p is concrete resistivity at each location [kΩ].

The method to convert the half-cell potential applied by Eq. (11) is named the inversion by BEM (IBEM)

3. Experiment

3.1. Specimens

One type of specimen was casted for an RC slab of 100 mm×570 mm×1010 mm. Two different types of specimens were fabricated. One is a non-crack type on the surface, and the other is cracked one on the surface. Two steel plates with a dimension of 3 mm×25 mm×466 mm were inserted to simulate cracks as shown in Fig. 3. Rebars with a 16 mm diameter were embedded by 50 mm in a thick cover as shown in Fig. 3.

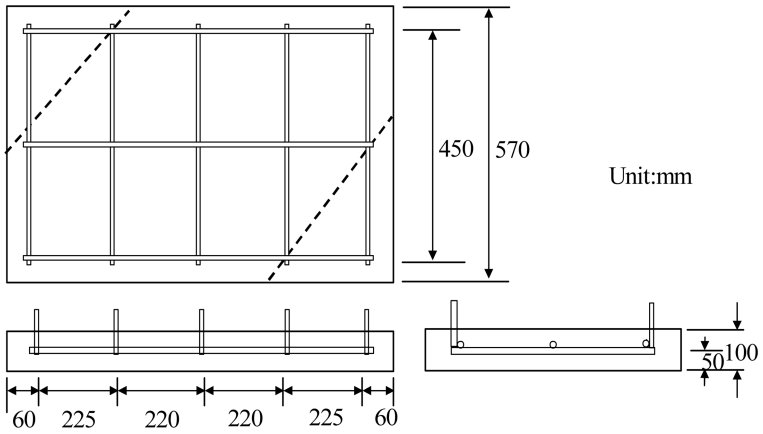

(a) Specimen of the crack type on the surface

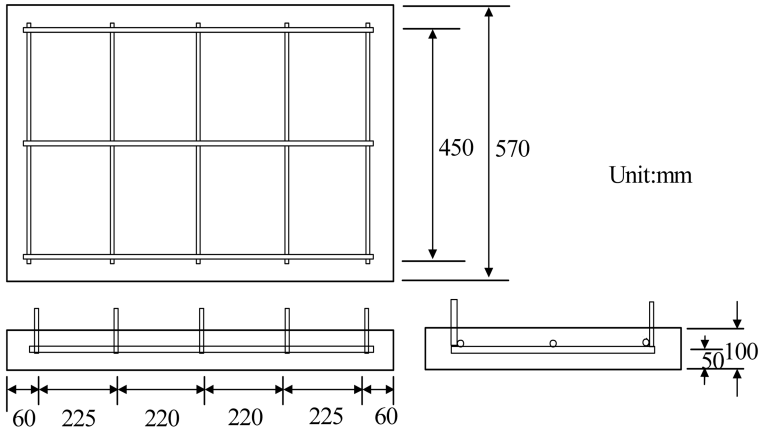

(b) Specimen of the non-crack type on the surface

Fig. 3 Arrangement of rebars and cracks

To accelerate corrosion, a half portion of 3% NaCl solution by water weight was mixed according to the model. In Fig. 3, the left half portion of the specimen in the plan view was casted with 3% NaCl and right half with only water. The mixture proportion of concrete is given in Table 1. The uniaxial compressive strength of concrete was 40.2 MPa at 28 days. The specimens were moisture-cured at 20°C for 28days. After removing it from the mold, the top surface of each specimen and rebar surface were coated by epoxy for protecting it from corrosion.

Table 1 Mixture proportion of concrete

Maximum gravel size (mm)	W/C (%)	Weight for unit volume(kg/m³)				NaCl/W (%)	Slump (cm)	Air (%)
		Water	Cement	F.A	C.A			
20	50	172	346	807	1054	3.0	4.9	5.2

3.2. Accelerated corrosion test

Rebars in concrete were artificially corroded through an accelerated corrosion test for 0 hr, 18 hrs, 24 hrs, and 36 hrs, respectively. The test set-up and RC slab with surface cracks are shown in Fig. 4. A copper plate was placed on the bottom of a tub. The specimen was mounted on the copper plate, and a 3% NaCl solution was filled to the surface of the specimen. By supplying currents, a constant 300 mA electric current was charged between the rebars and the copper plate.

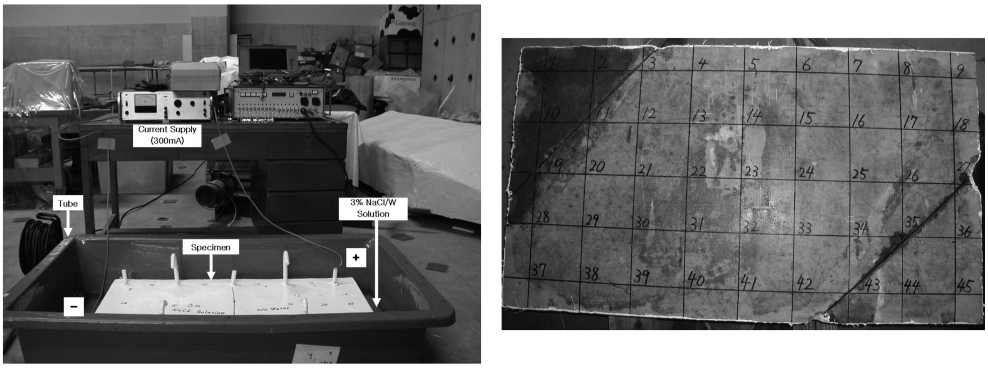

Fig. 4 Set-up of accelerated corrosion test and RC slab

3.3. Measurement

Half-cell potentials, concrete resistance, and polarization resistance at the concrete surface were measured by using a portable corrosion meter (SRI-CM-III) (Yokota 1998, 1999, Yokota, *et al.* 2008). As shown in Fig. 5, the equipment is based on an AC impedance method and uses a three-electrode system. Concrete resistivity and polarization resistance are measured by central counter electrodes. With the advantage of a double-disk counter electrode system, the guard electrode can confine the scattering of currents within the central electrode. The half-cell potential was also measured.

For the measurement of the polarization resistance, a small sinusoidal voltage is applied. Also, the amplitude of sinusoidal current response and the phase difference between the two signals were measured. The apparent polarization resistance, R'_{ct} , was obtained from the AC impedance measurements at two frequencies of 10 Hz and 20 mHz. Then, the true polarization resistance, R_{ct}, was defined by

$$R_{ct} = R'_{ct} \times S \tag{1}$$

where R'_{ct} is apparent polarization resistance, and S (= 82 cm^2) is the surface area of a steel rebar. The polarization resistance is in an inverse proportion to the corrosion current density, Icorr, which is defined from the formula developed by Stern and Geary.

$$I_{corr} = \frac{K}{R_{ct}} \tag{2}$$

where the value of K is assumed to be 0.026V.

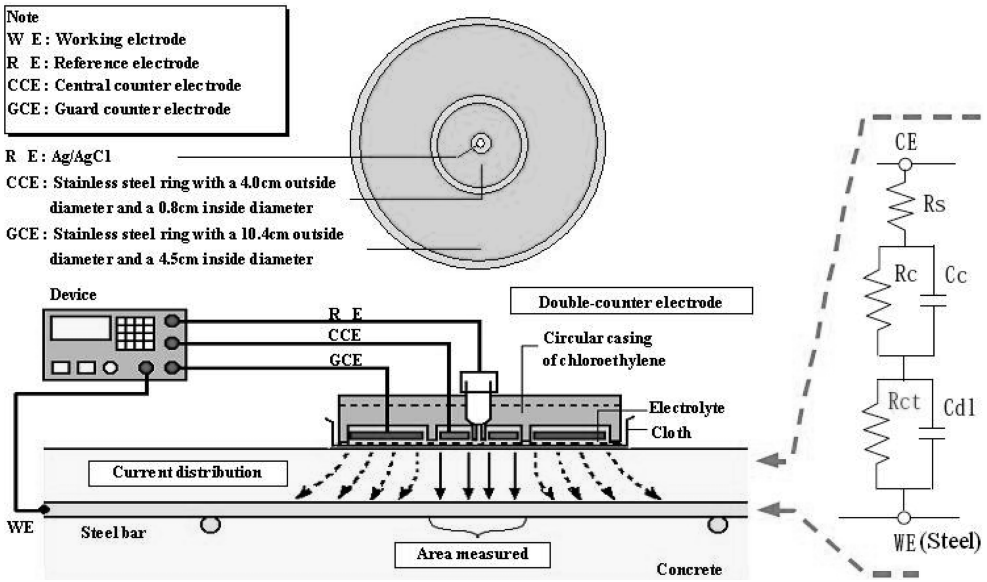

Fig. 5 Measurement using a double-counter electrode

The measurement was conducted by 30 minutes after the current drive was stopped to stabilize the electro-chemical reaction, and the specimen was taken out of the tub.

3.4. Three-dimensional illustration

VRML is a type of Virtual Reality Modeling Language that makes a virtual space in display. All the data measured was transferred to a microcomputer, and all results were displayed on a CRT by employing the VRML (Kyung, *et al.* 2005). Thus, geometrical and electrical information on the measuring points could be entirely displayed. The criterion for the half-cell potential (mV vs. CSE) based on ASTM C876 is given in Table 2.

3.5. Corrosion area

To inspect corrosion in the specimens, the concrete cover was removed after the test. Then, the corrosion area was calculated using an automatic area measuring instrument after drawing corrosions on the rebars using tracing paper and coloring the corroded portion in black as illustrated in Fig. 6.

Table 2 Criterion for half-cell potential (mV vs. CSE) based on ASTM C876

Potential value	Criterion	Color of rebar
-200 mV < E	No corrosion	White
-350 mV < E ≦ -200 mV	Uncertain	Orange
E ≦ -350 mV	Active corrosion	Red

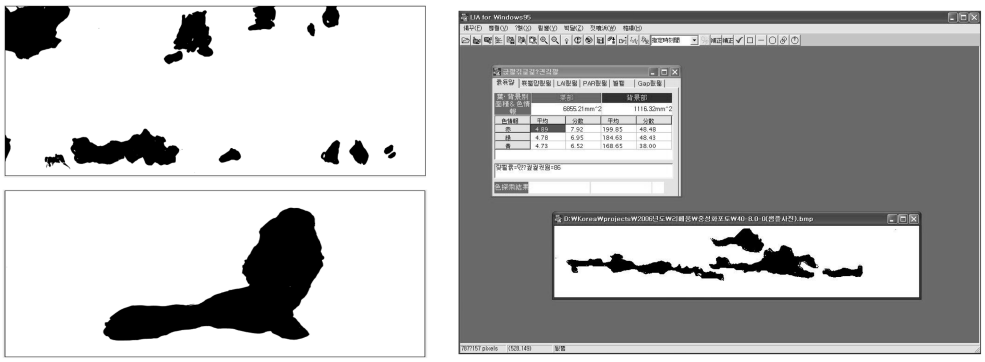

(a) Tracing papers of corrosion area (b) Area measuring instrument

Fig. 6 Corrosion area and automatic area measuring instrument

(a) Level 1 (b) Level 2 (c) Level 3

Fig. 7 Degree of corrosion

3.6. Visual inspection and corrosion levels

To inspect corrosion in the specimens, the concrete cover was removed after the test. Then, the rebar corrosion was rated according to the three corrosion levels as illustrated in Fig. 7. Level 1 represents no visible rusts on the surface. Level 2 shows a little rust on the surface. Level 3 indicates heavy corrosion. It was not worth that this corrosion rating was based on visual inspection on the surface of the rebars in which the pitting corrosion was not taken into account because it was difficult to observe by the naked eye (Qian, *et al.* 2005).

4. Results

4.1. Concrete resistivity

All data was measured at 45 points of which locations are denoted in Fig. 2. All measurements were conducted after the specimen was taken out of the tub and elapsed for 30 minutes because the accelerated corrosion test was adapted. Variations in concrete resistance before and after accelerated corrosion tests are shown in Fig. 8. In the specimen with surface cracks, variations in concrete resistance were found to be inhomogeneous relatively. Consequently, regarding the coefficient of concrete resistance, R was calculated by Eq. (12). The results of the test are summarized in Table 3. The average value R_{ave} is equal to 0.650 kΩ. Thus, half-cell potentials on rebars were compensated by using the concrete resistance in Table 3.

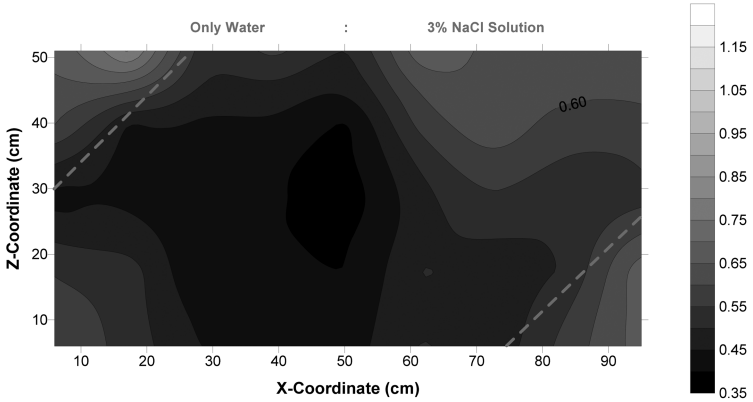

(a) Before accelerated corrosion test

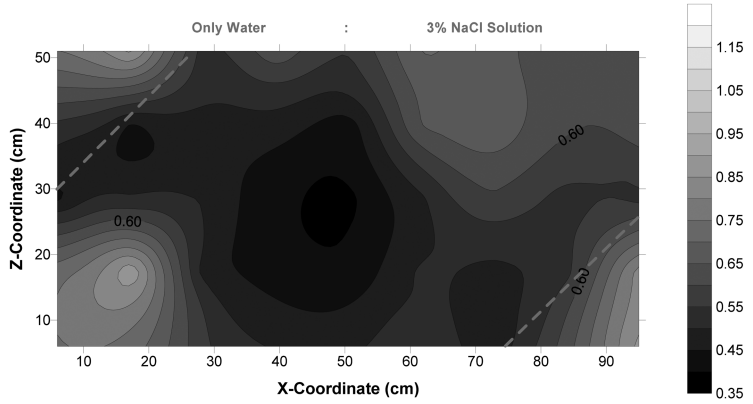

(b) After a 18hr accelerated corrosion test

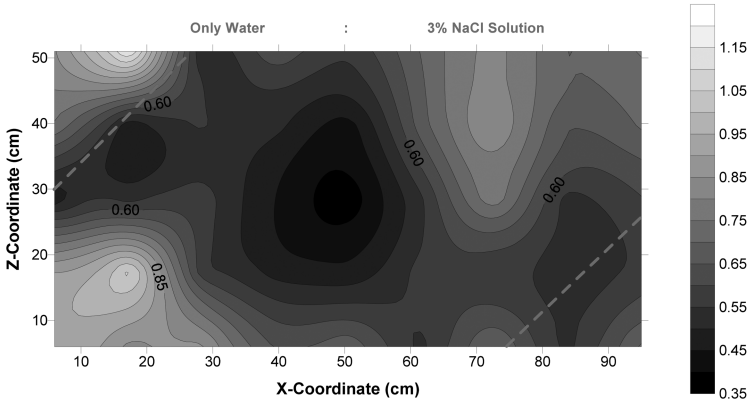

(c) After a 36hr accelerated corrosion test

Fig. 8 Variation of concrete resistance by an acceleration corrosion test (kW)

Table 3 Relative coefficients of concrete resistance:R_{ave} = 0.650 kΩ

No.	1	6	11	16	21	26	31	36	41
R_p	0.844	0.702	0.448	0.851	0.575	0.534	0.480	0.563	0.690
R	0.770	0.925	1.450	0.763	1.130	1.216	1.353	1.154	0.941

4.2. Polarization resistance and half-cell potentials

Variations in polarization resistance before and after accelerated corrosion tests are shown in Fig. 9. It is found that variations in polarization resistance and concrete resistance were found to be

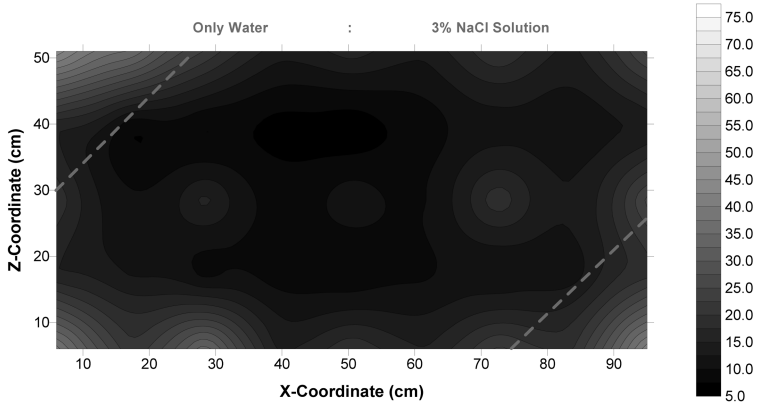

(a) Before accelerated corrosion test

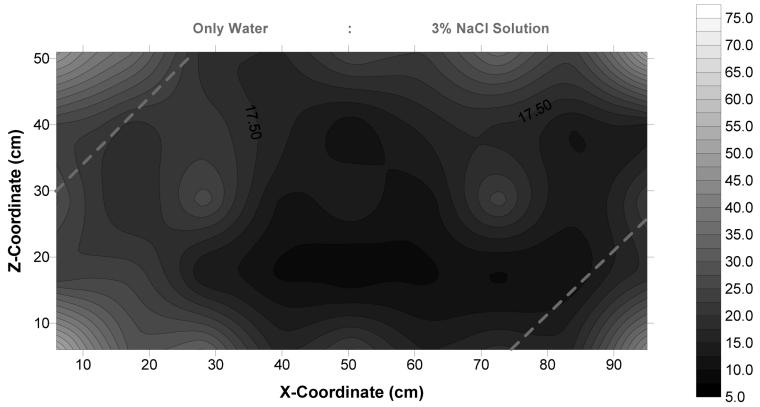

(b) After a 18hr accelerated corrosion test

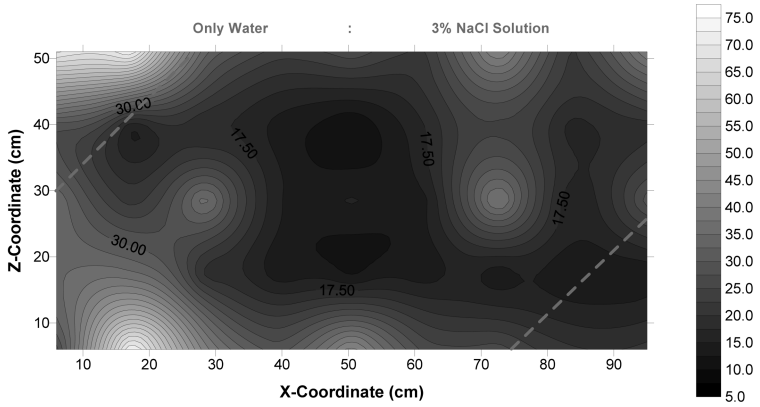

(c) After a 36hr accelerated corrosion test

Fig. 9 Variation of polarization resistance by an accelerated corrosion test ($k\Omega \cdot Ecm^2$)

inhomogeneous relatively in the specimen with surface cracks. Then, the polarization resistance was sensitive to concrete resistance in RC slabs.

A contour map of the potentials observed in the RC slabs with cracks before and after employing an accelerated corrosion test for 36 hrs is shown in Fig. 10.

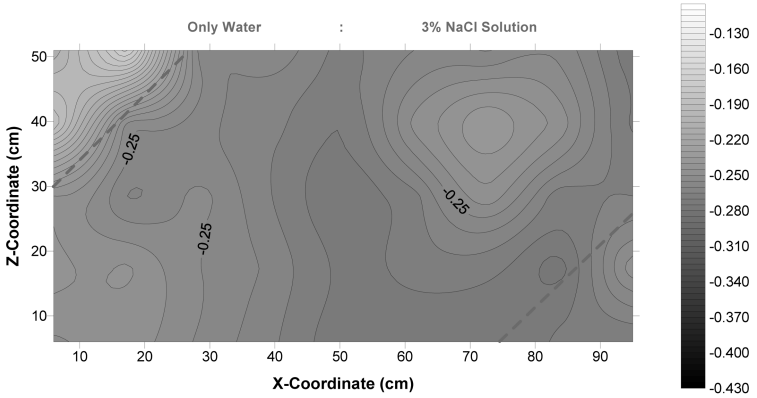

(a) Before accelerated corrosion test

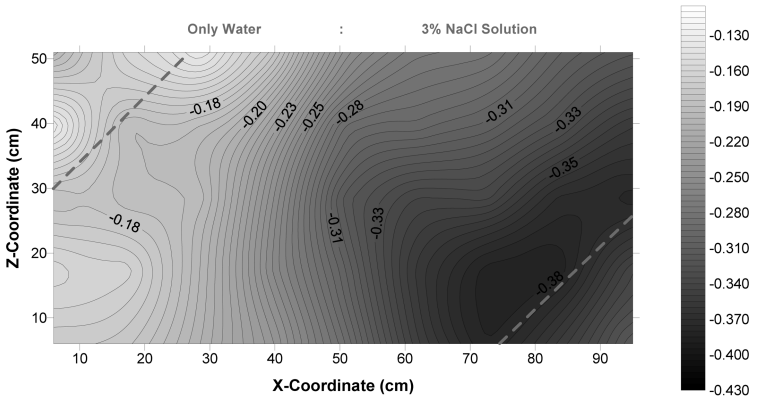

(b) After a 18hr accelerated corrosion test

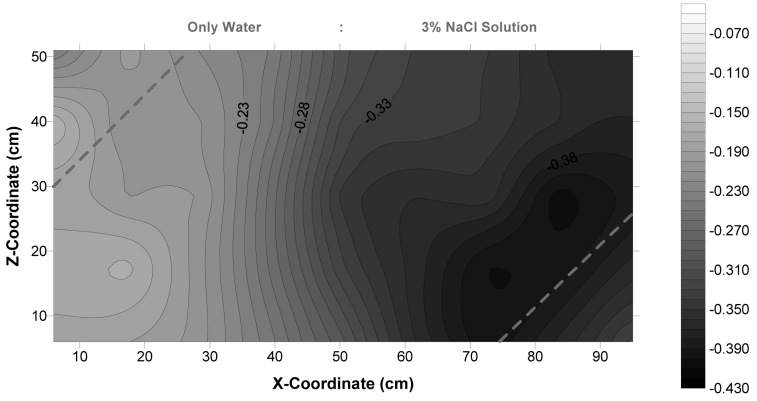

(c) After a 36hr accelerated corrosion test

Fig. 10 Variation of potentials by an accelerated corrosion test (V vs. C.S.E)

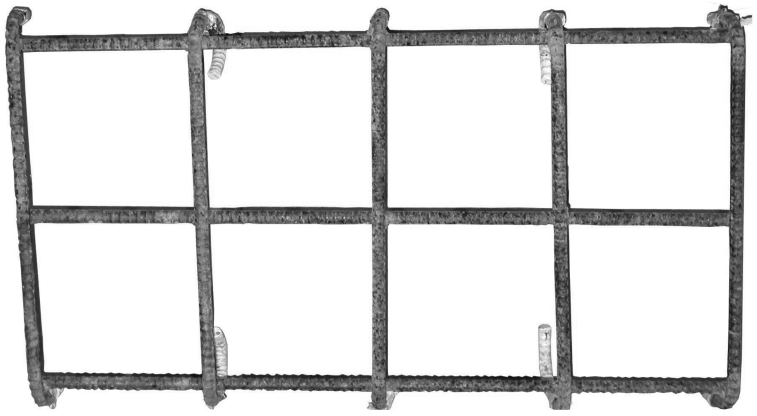

(a) Corrosion situation of rebar after accelerated corrosion test

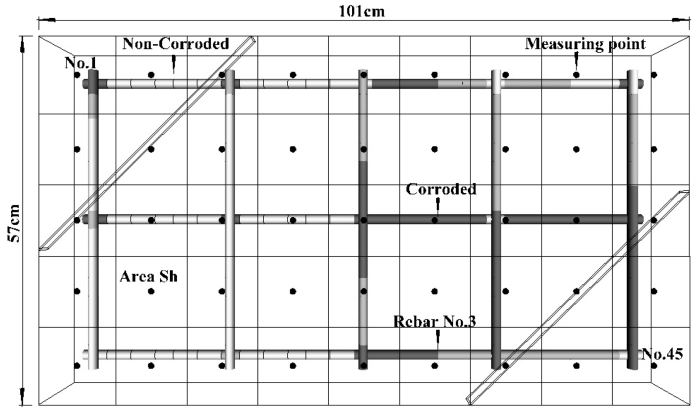

(b) Results of visual inspection by VRML

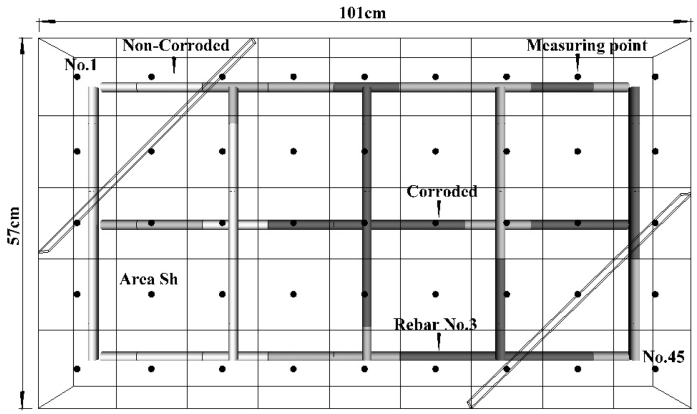

(c) Results of IBEM

Fig. 11 Results of half-cell potential measurement in specimen with surface cracks

The criterion for the half-cell potential (mV vs. CSE) based on ASTM C876 (1991) is given in Table 2. It implies that only rebars at the right portion are corroded.

After completing the measurements, the specimens were broken, and the rebars were removed to

Table 4 Rebar surface and corrosion area

	Water mixed portion		3% NaCl mixed portion	
	Non-crack part	Crack part	Non-crack part	Crack part
Rebar surface(mm^2)	132633.6	13816.0	132633.6	13816.0
Corrosion area(mm^2)	13263.4	1851.3	25642.5	5277.7
Rate of corrosion area (%)	12	14	26	40

identify the corroded areas. The corrosion situation of rebars after applying accelerated corrosion tests for 36 hrs is shown Fig. 11(a). In Fig. 11(b), the corrosion situation of rebars is classified by color and by VRML. By applying Eq. (11), the potential at rebars was computed, and then the ASTM criterion was applied to the potential at the rebars. Then, the results are given in Fig. 11(c) by VRML. Reasonable agreement between the actual corroded region and the estimated region was observed.

Since the procedure for the compensation provides direct information regarding potentials on the rebars, it can be applied to precisely identify corroded regions of the rebars. Thus, a reliable procedure to identify corroded regions of rebars was developed.

4.3. Corrosion areas

After finishing the accelerated corrosion test, the specimen was crushed to take out the rebars from the concrete. The corrosion area was calculated using an automatic area measuring instrument after copying the rusts on the rebars using tracing paper and coloring the rusted portion in black in Table 4. In spite of a difference of mixture water, the corrosion area of the crack part is larger than non-crack part. Because it is easily to penetrate the chloride ion to the surface of reinforced rebars by influence of the crack. The corrosion area that already had more parts of chloride ions, 2 to 4 times, than the part of pure water occurred due to macro-cell corrosion environment.

5. Conclusions

A compensation procedure for the half-cell potential measurement was investigated, and an IBEM analysis was developed. The procedure converted the potential on concrete surface to those on rebars or at the interface with rebars. The applicability was examined by applying accelerated corrosion tests for RC slabs. Also, the results obtained in this test are summarized as follows:

(1) It is found that the polarization resistance is sensitive to concrete resistance.

(2) By applying the IBEM analysis, the potential at rebars were computed. Then, the ASTM criterion was applied to estimate corrosion. To take into account the crack in concrete, the relative coefficient of concrete resistance was introduced to the analysis.

Acknowledgement

This study was supported by the Sustainable building research center(SUSB) of Hanyang University (R11-2005-056-04003) that is the SRC/ERC program sponsored by the Ministry of Education, Science and Technology.

References

Andrade, C. and Alonso, C. (2001), "On-site measurements of corrosion rate of reinforcements", *Constr. Build. Mater.*, **15**(2), 141-145.
ASTM C876 (1991), *Standards Test Method for Half Cell Potentials of Reinforcing Steel in Concrete*.
Brebbia, C.A. (1978), *The Boundary Element Method for Engineers*, Pentech Press Ltd., London.
Chris, M. and Bruce, C. (1997), *Teach yourself VRML2 in 21 days*, San·Enet, NY.
Dubravka, B., Dunja, M., and Dalibor, S. (2000), "Non-destructive corrosion rate monitoring for reinforced concrete structures", *Proceedings of 15th WCNDT*, Roma, October.
Fontana, G.. (1987), *Corrosion Engineering.* McGrawHill, NY.
Hartman, J. (1996), *VRML 2.0 Handbook*, Addison-Wesley, NY.
Hietpas, K., Ervin, B., Banasiak. J., Pointer, D., Kuchma, D.A., Reis, H., and Bernhard, T. (2005), "Ultrasonics and electromagnetics for a wireless corrosion sensing system embedded in structrual concrete", *Smart Struct. Syst.*, **1**(3), 267-282.
Jaggi, S., Bohni, H., and Elesner, B. (2001), "Macrocell corrosion of steel in concrete-experiments and numerical modelling", *Proceedings of Eurocorr 2001*, Milan, September.
Kyung, J.W. Tae, S.H. Lee, H.S. Alver, Y., and Yoo, J.H. (2007), "IBEM analyses on half-cell potential measurement for NDE of rebar corrosion", *Comput. Concrete*, **2**(4), 285-298.
Kyung, J.W., Yokota, M., Leelalerkiet, V., and Ohtsu, M. (2005), "Visual reality presentation for nondestructive evaluation of rebar corrosion in concrete based on inverse BEM", *The Korean Society for Nondestructive Testing,* **25**(3), 157-162.
Lee, H.S. Kage, T. Noguchi, T., and Tomosawa, T. (2003), "An experimental study on the retrofitting effects of reinforced concrete columns damaged by rebar corrosion strengthened with carbon fiber sheets", *Cement Concrete Res.*, **33**, 563.
Maurel, O. (2005), "Relation between total degradation of steel concrete bond and degree of corrosion of rc beams experimental and computational studies", *Comput. Concrete*, **2**(1), 1-18.
Okada, K. Kobayashi, K., and Miyagawa, T. (1988), "Influence of Longitudinal cracking due to reinforcement concrete members", *ACI Mater. J.*, **85**, 134.
Qian, S.Y. and Chagnon, N. (2001) "Evaluation of corrosion of reinforcement in repaired concrete", Structural Faults and Repair, London, UK.
Tae, S.H., Kyung, J.W., and Ujiro, J. (2006), "Service life estimation of concrete structures reinforced with cr-bearing rebars under macrocell corrosion conditions induced by cracking in cover concrete", *The Iron and Steel institute of Japan International,* **47**(6), 875-882.
Yokota, M, Kyung, J.W., and Lee, H.S. (2008), "Environmental influence on the corrosion rate of steel bars embedded in concrete", *The Iron and Steel institute of Japan International*, **48**(2), 230-234.
Yokota, M. (1998), "Corrosion rate measurements of reinforcing bars in real concrete structures using ac impedance method", *Proceeding 7th European Conference on NDT*, Copenhagen, May
Yokota, M. (1999), "Study on corrosion monitoring of reinforcing steel bars in 36-year-old actual concrete structures", *Concrete Library of JSCE,* **33**, 154-164.

CC